Journal of Materials Chemistry A

REVIEW

View Article Online
View Journal | View Issue

Cite this: J. Mater. Chem. A, 2016, 4, 4353

Influence of the composition of hybrid perovskites on their performance in solar cells

Josep Albero,[a] Abdullah M. Asiri[b] and Hermenegildo García*[a]

During the last 5 years, power conversion efficiencies of hybrid (organic–inorganic) halide perovskite solar cells have shown impressive advances. This success has been partly due to the advances in thin film deposition techniques, but also due to the understanding of the chemical and structural characteristics of the hybrid organic–inorganic perovskites that make it possible to modulate their optoelectronic properties. Moreover, engineering the chemical composition of these materials still remains a powerful tool for further improvement of the photovoltaic activity of these materials. The preparation of efficient lead-free hybrid perovskites exhibiting reduced toxicity is one of the main targets. Besides environmental issues, the control of the composition of hybrid perovskites should be used to achieve a decrease in the bandgap energy, trying to extend the photoresponse of the materials into the NIR region. A third target is the long-term stability of devices, a property closely related to the negative influence of humidity and phase transition. This review focuses on showing how the modification of the composition of each of the three components (organic cation, metal and inorganic anion) of the parent hybrid halide perovskite ($CH_3NH_3PbI_3$) influences the optoelectronic properties, photovoltaic efficiency and stability of these striking materials.

Received 12th January 2016
Accepted 8th February 2016

DOI: 10.1039/c6ta00334f

www.rsc.org/MaterialsA

[a]Instituto Universitario de Tecnología Química CSIC-UPV, Univ. Politécnica de Valencia, Avda. De los Naranjos s/n, 46022, Spain. E-mail: hgarcia@qim.upv.es; Tel: +34 963877807

[b]Center of Excellence for Advanced Materials Reseach, King Abdulaziz University, Jeddah, Saudi Arabia

Josep Albero was born in 1980. He obtained the Chemical Engineering degree from the Jaume I University of Castellon (Spain) in 2005. Later he obtained his M.Sc. degree from Rovira I Virgili University in 2009. He worked in the synthesis and characterization of nanocrystalline semiconductor quantum dots for photovoltaic applications when he received his PhD in the group of E. Palomares at ICIQ. Afterwards he joined the H. Garcia group in ITQ as a postdoctoral fellow. His research interests are the charge transfer reactions in nanostructured materials and their applications in renewable energies.

Abdullah M. Asiri received his PhD from the University of Wales, College of Cardiff, UK, in 1995. He has been the Head of the Chemistry Department at King Abdulaziz University since October 2009 and he is the founder and the Director of the Center of Excellence for Advanced Materials Research. He is a Professor of Organic Photochemistry. His research interests cover color chemistry, synthesis of novel photochromic, thermochromic systems, synthesis of novel coloring matters and dyeing of textiles, Materials Chemistry, Nanochemistry and Nanotechnology Polymers and plastics. He is the Editor-in-Chief of King Abdulaziz University Journal of Science. He is also a member of the Editorial Board of Pigments and Resin Technology (UK), Organic Chemistry in Sight (New Zealand), Designed Monomers & Polymers and Journal of Single Molecule Research. He is the Vice-President of Saudi Chemical Society (Western Province Branch). He has co-authored over 500 papers and three book chapters and holds three international patents.

Introduction

Organic–inorganic perovskite solar cells have erupted in the field of photovoltaics with such an impetus that according to data extracted from the Web of Science the number of publications in the last few years has grown exponentially, going from less than 20 in 2012 to more than 220 in 2014, receiving more than 5000 citations in that year, and it can be foreseen that this tendency will continue at an increasing pace in the following years. The considerable attention on hybrid (organic–inorganic) perovskite technology has arisen from the fast power conversion efficiency improvements that this material has achieved in photovoltaic devices. Since the first report in 2009 where 3.8% efficient devices were reported for $CH_3NH_3PbI_3$ perovskites as an inorganic sensitizer in photoelectrochemical solar cells using an I^-/I_3^- liquid electrolyte,[1] remarkable efficiency records have been continuously attained in short intervals, this evolution contrasting favorably with conventional dye-sensitized solar cells. The substitution of liquid electrolytes by solid state hole conductors such as spiro OMeTAD (2,2′,7,7′-tetrakis-(*N*,*N*-di-4-methoxyphenylamino)-9,9′-spirobifluorene) pushed rapidly efficiencies up to 8%, overcoming the negative effect of perovskite solvation in acetonitrile. Moreover, the use of a mesoporous Al_2O_3 layer instead of an n-type TiO_2 semiconductor increased even higher the device efficiency up to 10.9% using the mixed halide $CH_3NH_3PbI_3(Cl)$ in 2012.[2] Continuous progress has been made since then, combining adapted film processing conditions with material design, resulting in efficient devices up to 19.3% (from a reverse-bias current–voltage curve) presented in 2014.[3] More recently, researchers in the Korea Research Institute of Chemical Technology (KRICT) presented a certified perovskite solar cell of 20.1% that is probably the current efficiency record at this moment.[4] Consequently, perovskite solar cells are nowadays serious competitors to the thin film technologies based on semiconductor chalcogenides such as CdTe or copper indium gallium selenide (CIGS).

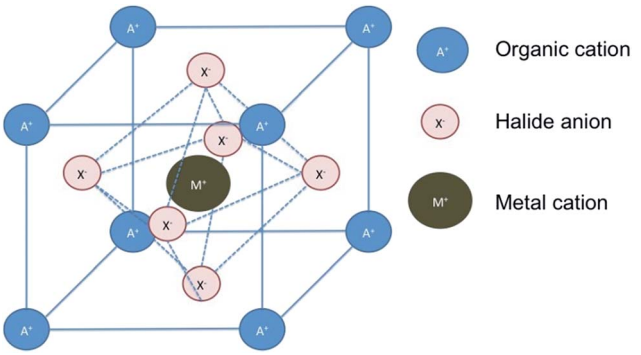

Scheme 1 General crystal structure of a typical hybrid perovskite.

Intensive research has been carried out to determine the properties of the hybrid halide perovskite as a function of the composition. The general chemical formula of perovskites follows a AMX_3 pattern, where A (smaller) and M (larger) represent two cations of different sizes, A being organic in the present case, and X an anion (Scheme 1). This general formula allows a large variety of compositions, including oxides, nitrides or halides, which may form different crystalline phases (cubic, tetragonal or orthorhombic) and structures (3D or 2H), including distorted structures (Scheme 2). As a consequence of this variety of compositions and structures, perovskites exhibit a wide range of physical and chemical properties such as ferro- and piezoelectricity, magnetism, superconductivity, semiconductivity and catalytic activity.

There have been two main reasons for these significant performance improvements in such a short period of time. On one hand, the formation of dense, high quality, continuous and crystalline thin films of organic–inorganic perovskites, through

Hermenegildo García is a full Professor at the Instituto de Tecnología química of the Technical University of Valencia, a joint center of the Technical University of Valencia and the Spanish National Research Council and a Honorary Adjunct Professor at the Center of Excellence in Advanced Materials Research of King Abdulaziz University. He made a post-doctoral stay at the University of Reading with Professor Andrew Gilbert and several sabbatical leaves in the group of Professor J. C. Scaiano at the University of Ottawa. Prof. Garcia has been active in the field of heterogeneous catalysis working with porous catalysts and nanoparticles, has published over 600 papers and has filed over 25 patents. Prof. Garcia is doctor Honoris Causa from the University of Bucharest and the recipient of the 2011 Janssen-Cilag award given by the Spanish Royal Society of Chemistry and the 2008 Alpha Gold of the Spanish society of Glass and Ceramics.

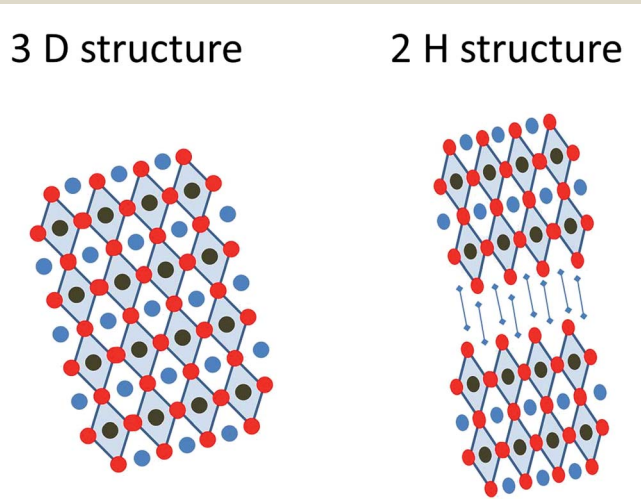

Scheme 2 Pictorial illustration of the 3D and 2H structures of a perovskite.

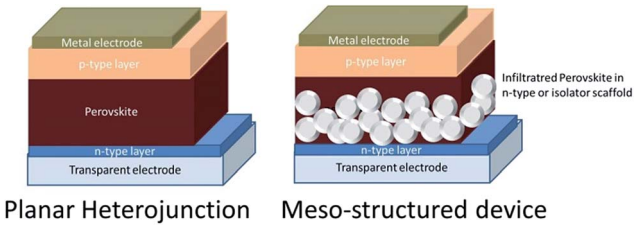

Scheme 3 Illustration of the two main hybrid perovskite solar cell architectures.

optimized processing chemistry.[3,5,6] On the other hand, optimization of the composition of the material by incorporation of different organic cations (A), metal cations (M) and halide anions (X) into the perovskite composition has been a second strategy to increase solar cell efficiency.[7,8] This composition optimization constitutes the focus of the present review.

Two device architectures have been extensively used in perovskite solar cells: the planar heterojunction and the mesostructured cell (Scheme 3). In the first case, a flat perovskite layer is sandwiched between selective n- and p-type semiconductors, while in the second case, perovskites are infiltrated into a mesoporous layer which can be either an n-type semiconductor material or an insulator which acts as a rigid matrix. In both cases, several methodologies have been developed to fabricate notably efficient hybrid halide perovskite solar cells.

The easiest method for device preparation is based on the straightforward formation of most common hybrid perovskites and consists of one step deposition, in which two precursors, the metal halide and the organic halide, in a common organic solvent, are mixed together and subsequently deposited on a substrate by spin coating (Scheme 4). This method has been used both for solar cells based on planar surfaces and mesoporous layers, but is particularly suitable for perovskite deposition in mesoporous layers. Initial reports state that spin coating directly onto compact, flat substrates in planar heterojunction architectures resulted in unsatisfactory surface coverage and, therefore, in poor device performance as well as low device reproducibility due to dewetting effects.[9] It has been widely reported that device performance strongly depends on the film morphology. This is a consequence, on one hand, of the inefficient charge carrier transport and diffusion length which may produce losses on the current density of the devices at short circuit.[10,11] On the other hand, inappropriate film morphology promotes the presence of defects in the film and crystal grain boundaries which act as carrier traps, enhancing recombination events as well as hysteresis effects, which causes inaccuracy in the characteristic *I–V* measurements.[12,13] Morphology control was improved through careful processing condition optimization. Inert processing environments, optimized spin coating conditions and adequate annealing temperature control allowed improvements in film morphology and, therefore, the efficiency of devices was enhanced.[6] In addition, composition engineering by precursor selection [*i.e.* $PbCl_2$, PbI_2 or $Pb(OAc_2)$] was found to be crucial to obtain faster and more uniform crystallization during deposition, thus, improving the device efficiencies up to 14% by using $Pb(OAc)_2$ as the precursor.[6] Despite the improved film properties that processing conditions and composition engineering have achieved in the one step deposition method, still some variations in the film thickness have been found,[14] leading to low reproducibility of efficiency of these devices. In contrast, more uniform perovskite films have been achieved using dual source coevaporation of the precursors[14] (Scheme 4). Solvent engineering has been also proposed as an effective method in order to improve the film morphology. In this regard, solvent mixtures of dimethylsulfoxide and γ-butyrolactone have been employed in the preparation of $CH_3NH_3Pb(I_{1-x}Br_x)_3$ perovskites followed by toluene drop casting. This procedure yielded extremely uniform and dense perovskite layers due to the formation of a more stable phase that retards the fast $CH_3NH_3I(Br)$ and $PbI(Br)_2$ reaction.[15] In a similar way, Park and coworkers described the formation of a 1 : 1 : 1 adduct of CH_3NH_3I–PbI_2–DMSO by spin coating on DMF solution and subsequent diethyl ether addition to remove the excess of less-volatile solvents.

In this way, they obtained highly efficient (~19%) and reproducible perovskite solar cells.[16]

Improved particle morphology control has been achieved through a two-step deposition method (Scheme 4). In this method, the metal halide precursor is deposited either in the mesoporous layer or on the flat substrate. After an annealing treatment, the metal halide layer is exposed to the organic halide precursor by soaking the supported metal halide layer in an organic halide solution[17] or by exposing the film to the precursor vapor.[18]

A two-step method in which the two precursor materials were sequentially spin coated one on top of the other has been also reported and the perovskite formation is achieved by reactant diffusion.[19,20]

The systematic morphology control of the perovskite films that can be achieved with the deposition technologies has provided comprehensive understanding of the nucleation and growth steps occurring in the perovskite formation, and this information has been very useful for device optimization. For further detailed coverage of the perovskite crystal growth methods and reported deposition techniques the reader should refer to the existing literature in this topic.[5,6,8,21–23]

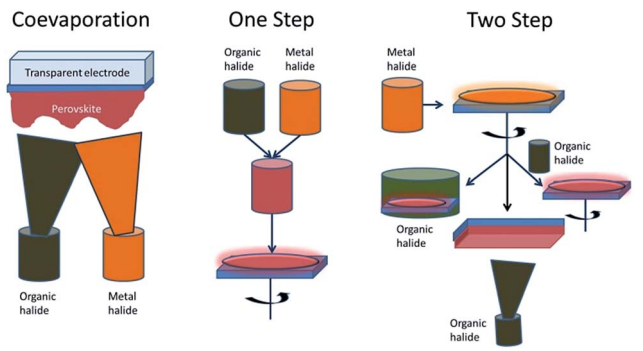

Scheme 4 Three general methodologies, coevaporation, one step solution method and two step solution methods, employed for the deposition of hybrid perovskites.

Besides selection of the adequate film formation technique, further improvements can be achieved through design and careful control of the hybrid perovskite composition and by improvement of the synthetic procedures. In this review, we have focused on the influence on the device performance derived from the systematic substitution of organic and metal cations or halide anions in the prototypical $CH_3NH_3PbI_3$ perovskite.

In spite of the efficiency enhancement due to the reduced light losses and optimized optical and electronic properties achieved through improved processing with the parent $CH_3NH_3PbI_3$ perovskite, some remaining important issues that cannot be solved by film formation are still under discussion. Firstly, the search for lead-free nontoxic perovskites is one of the main objectives in order to introduce this type of photovoltaic cell in the commercial market without causing environmental concerns. A second point is to extend the spectral response of the photoactive perovskite towards the NIR part of the spectra to harvest the maximum possible sunlight. A third crucial problem to be solved is the ambient condition instability exhibited by $CH_3NH_3PbI_3$ perovskite. The main instability issue arises from the moisture sensitivity that this material presents. Therefore, new strategies in the composition are desirable in order to obtain moisture stable perovskites. Moreover, it has been reported that the other instability source could arise from the phase transition from the tetragonal to the cubic structure that typically takes place at about 330 K for this material.[24] Therefore, perovskite compositions having a tetragonal structure and improved stability are also highly desirable. Other properties to be improved by suitable composition optimization are the crystal size and phase, bandgap tuning, recombination control, charge transport properties and reduction of the *J–V* hysteresis.

Among all perovskite compositions, hybrid organic–inorganic perovskites and their derivatives have come under the spotlight in photovoltaics during the last few years due to the excellent optical and electronic properties that they have demonstrated, boosting device efficiencies up to 20% under 1 Sun illumination. The AMX_3 composition is retained in these hybrid perovskites, A being an organic cation. The most employed perovskite in photovoltaic applications corresponds to a 3D structure perovskite formed by methyl ammonium as an organic cation, lead as a metal and iodine as an inorganic anion ($CH_3NH_3PbI_3$). Nevertheless, several alternatives for each one of the different components (A, M and X) of these hybrid perovskites have been explored with the aim of overcoming the existing limitation in the field. In the following sections, we will describe the different composition alternatives to the archetypical $CH_3NH_3PbI_3$ perovskite widely employed in photovoltaics and their impact on the photoresponse and stability of the resulting material.

The organic cation

It is well established that the organic cation in hybrid perovskites determines the perovskite structure and dimensionality, influencing some optoelectronic properties as well as the perovskite stability. The cation size can be responsible for lattice expansion or contraction, leading to bandgap modification (Scheme 5). This

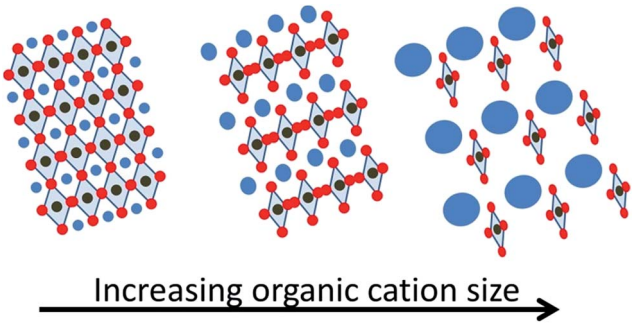

Scheme 5 Pictorial illustration of the lattice expansion with the organic cation size.

is a consequence of the four edge-sharing MX_6 octahedra, which only allow small cations into the 3D perovskite structure. In fact, a tolerance factor has been applied in order to define the limits on ionic sizes of each component.[25] Theoretical calculations have predicted that different organic cations, in addition to contributing to the structural distortion of the inorganic octahedra because of their size, affect the crystal structure due to the electrostatic interaction between the acidic hydrogens in the organic cation and the inorganic halogens, through hydrogen bonding, promoting a red-shift in the absorption onset and improving the charge transport properties of these devices.[26] Nevertheless, $CH_3NH_3^+$ with an ionic radius of 0.217 nm has been the most employed cation and some of the best device performances have been reported comprising always this organic cation in the hybrid perovskite composition.[7] However, other organic cations with a larger or smaller radius have been also reported. The interest in replacing $CH_3NH_3^+$ by different cations comes from, on one hand, the well-known undesirable moisture sensitivity of $CH_3NH_3PbI_3$ and, on the other hand, from the reversible phase transition of this perovskite composition between tetragonal and cubic at 57 °C.[24] This temperature usually falls within the device operating temperature, affecting the band structure and, therefore, the photovoltaic performance and stability. Perovskites lacking this unwanted phase transition under operation should be preferred.

Additionally, the use of different organic cations (*i.e.* formamidium, $HC(NH_2)_2^+$) instead of $CH_3NH_3^+$ in planar heterojunctions improves the cell performance by showing negligible hysteresis between forward and reverse *J–V* measurements.[5,27,28]

Besides moisture sensitivity and the phase transition issue, the need to expand the light absorption towards the NIR region requires the reduction of the perovskite bandgap. The typical hybrid perovskite $CH_3NH_3PbI_3$ containing methyl ammonium cations possesses a 1.55 eV band gap, being the ideal bandgap estimated between 1.1 and 1.4 eV for a single-junction solar cell.[28] The CH_3NH_3I precursor is typically prepared by the reaction between a CH_3NH_2 solution in methanol or ethanol and a HI solution in water at low temperature for about 2 h.[8]

The utilization of other different organic cations could require adaptation of the synthetic method, although the organic halide cation preparation procedure has been used in the majority of the reports.

It is well known that the perovskite band gap is very sensitive to network structure modifications (*i.e.* deformation, enlargement or tilting). At room temperature, the tetragonal structure in $CH_3NH_3PbI_3$ is given by the small size of the $CH_3NH_3^+$ cation. Therefore, the incorporation of a bigger cation is believed to provide a higher symmetry to the perovskite structure and as a consequence, band gap reduction.[29]

In this regard, Nam-Gyu Park *et al.* reported the preparation of lead iodide perovskites of ethylamine ($CH_3CH_2NH_3PbI_3$) mixing equimolar solutions of ethylammonium iodide and lead iodide in γ-butyrolactone.[30] The $CH_3CH_2NH_3I$ was prepared by reacting an ethylamine solution in methanol with a hydroiodic acid solution in water, analogously to the typical methylammonium iodine preparation. The resulting perovskite presented a 2H structure consisting of PbI_6 chains separated one from the other by ethylammonium ions with an orthorhombic phase (see Scheme 2). The larger alkyl chain length in the organic cation does not allow maintaining the 3 D tetragonal AMX_3 lattice. As a consequence of the structural change, the perovskite bandgap increased up to 2.2 eV, and the power conversion efficiency using this cation in the lead iodide perovskite was lower than that of the methylammonium based perovskite.[30]

Similarly, Baikie and co-workers reported a perovskite containing a formamidium cation ($HC(NH_2)_2^+$, FA^+) instead of the methylammonium ($CH_3NH_3^+$). The ionic radius of FA^+ has been reported to be slightly bigger than that of the methylammonium ($r_{formamidium} = 0.279$ nm), and therefore the estimated formamidium based perovskite bandgap is 1.47 eV, allowing better spectral absorption.[31]

Pang *et al.* reported other synthetic routes for the $HC(NH_2)_2I$ preparation where formamidium acetate and HI reacted in water at 0 °C for 2 h. The as-prepared cation was used to build $FAPbI_3$ devices using a one-step solution process or the two-step dipping methodology. By using the latter method 7.5% efficiency was reported compared to only 3.7% efficiency obtained by the one-step deposition method. The reason for these results seems to be the feasibility of forming phase-pure $FAPbI_3$ following the two-step dipping method.[29]

In this context, Snaith *et al.* reported planar heterojunction devices containing this FA^+ based perovskite with an average efficiency of 9.7%.[28] In this case, the FAI precursor was prepared by dissolving an excess of formamidium acetate in a HI water solution. The halide perovskite was formed by adding an additional small amount of HI to the stoichiometric FAI : PbI_2 (1 : 1) in DMF solution during $FAPbI_3$ formation, observing the absence of the yellow phase after annealing. At the same time, Park *et al.* reported an improved FAI synthetic route, where high quality FAI was obtained with a yield above 90%.[27] The employed synthetic method does not use formamidium acetate as the precursor in order to avoid the formation of acetic acid during the reaction with HI which is not easy to eliminate. Instead of methanol they used ethanol in the presence of sodium hydride since in the formamidium formation, NaCl precipitation is favored due to the lower solubility of this salt in ethanol compared to methanol. Power conversion efficiencies up to 16% were obtained using $FAPbI_3$ perovskite prepared with the optimal precursor. Another additional advantage of this $FAPbI_3$ perovskite is that it does not show phase transition, increasing thermal stability when compared to the parent $CH_3NH_3PbI_3$.[27]

Seok *et al.* explored adequate solvents to form intermediate phases, thus retarding the reaction between PbI_2 and FAI. In this approach, the addition of DMSO as a co-solvent to the PbI_2 precursor was reported. The DMSO–PbI_2 precursor has been reported to promote the formation of more uniform and dense films. Subsequent exchange of DMSO by FA^+ cations was efficiently accomplished without structural changes due to their higher affinity for PbI_2, which provides highly uniform and dense $FAPbI_3$ films. Photovoltaic devices employing this DMSO–PbI_2 precursor and a subsequent intramolecular exchange process presented certified efficiencies exceeding 20%.[32]

A different approach was explored by Grätzel and co-workers who reported a systematic study on the partial substitution of the methylammonium cation by FA^+.[33] A maximum power conversion efficiency of 14.9% was obtained by using $(CH_3NH_3)_{0.6}FA_{0.4}PbI_3$. This combination produced a double benefit since the FA^+ cation not only reduced the perovskite bandgap, but also enhanced the light harvesting in the visible region by extending light absorption up to 850 nm. As a consequence, the $(CH_3NH_3)_{0.6}FA_{0.4}PbI_3$ perovskite based devices achieved photovoltages as high as those obtained for $CH_3NH_3PbI_3$, but with improved current densities. In a similar way, Han *et al.* reported a mix of methylammonium and 5-aminovaleric acid cations ($H_3N(CH_2)_4CO_2H^+$, AVA^+) in the synthesis of the mixed-cation perovskite $(5\text{-AVA})_x(CH_3NH_3)_{1-x}PbI_3$.[34] A certified power conversion efficiency of 12.8% was achieved by using this mixed-organic cation perovskite.

In this case, the partial substitution of the methylammonium cation by AVA^+ favors an orthorhombic perovskite phase, enhancing the light harvesting without a change in the spectral response, increasing the device photocurrent, and, therefore, the power conversion efficiency.

Recently, Seok *et al.* reported photovoltaic devices incorporating small proportions of ($CH_3NH_3PbBr_3$) into ($FAPbI_3$) to obtain $(FAPbI_3)_{1-x}(CH_3NH_3PbBr_3)_x$, where x varies from 0 to 0.3.[5] The rationale behind this strategy derives from the relative instability reported for $FAPbI_3$ due to the formation of a yellow non-perovskite polymorph (δ-phase) which should be responsible for inefficient charge transport and an increase in the optical bandgap. In contrast, $CH_3NH_3PbBr_3$ is well known to tune the perovskite band gap up to 2.3 eV as well as to stabilize the perovskite structure. By optimization of the molar ratio between $FAPbI_3$ and $CH_3NH_3PbBr_3$ to $x = 0.15$, the authors demonstrated stabilization of the perovskite black phase. The optimized phase stability and crystallinity enhanced the balance between electrons and holes in the perovskite, reducing the cell hysteresis and obtaining an average device efficiency between the reverse and forward applied bias of 18.4% under 1 Sun illumination.[5]

Although the best device efficiencies have been reported employing organic cations in the ABX_3 perovskite structure, some reports have questioned the need for using only organic cations.[35] In fact, it has been reported that Cs^+ doped

$CH_3NH_3PbI_3$ produced J_{sc} and V_{oc} improvements, enhancing the overall device efficiencies from 5.5 to 7.7%.[36] In this case, CsI was mixed with CH_3NH_3I in different proportions in order to form the final perovskite ($Cs_x(CH_3NH_3)_{1-x}PbI_3$) in the presence of PbI_2. The optimum device efficiency was obtained with a doping value of 10% of Cs^+. Further increase in Cs^+ content produced less efficient devices, not only due to bandgap enhancement, losing the spectral response, but also due to the presence of undesirable crystal phases such as CsI, PbI_2 and Cs_4PbI_6.[36]

Consideration of the current state of the art shows that there is still interest in testing other small size organic cations besides those containing N, preferably those that could give stable perovskite crystal phases, including in the study the most appropriate synthetic route for high purity perovskite formation and also a suitable film processing protocol. In addition, further understanding of the influence that doping with inorganic alkali metals and related cations can play in the performance of photovoltaic devices based on hybrid perovskites is still necessary.

The metal cation

It is well established that in the general formula (AMX_3) of hybrid organic–inorganic halide perovskites M corresponds to a divalent metal cation such as Cu^{2+}, Ni^{2+}, Co^{2+}, Fe^{2+}, Mn^{2+}, Cr^{2+}, Pd^{2+}, Cd^{2+}, Ge^{2+}, Sn^{2+}, Pb^{2+}, Eu^{2+} or Yb^{2+}.[37] The most studied divalent cations in photovoltaics have been Pb^{2+} and Sn^{2+}, although the most efficient devices have been obtained always using Pb^{2+}. Considering the toxicity of Pb^{2+}, replacement of this heavy metal cation by a less toxic metal that can result in an adequate perovskite bandgap without detriment to the performance of the photovoltaic device is at this moment under intense research. For this reason, group 14 elements with comparable ionic radii to that of Pb^{2+} have been intensely explored to allow replacement of toxic Pb.

Since the discovery of the electrical properties of inorganic oxide perovskites, a large number of compositions have been explored. One of the first reports on the synthesis and characterization of hybrid halide perovskites was carried out by Mitzi and co-workers in 1994.[38] They reported one family of hybrid halide perovskites ($(C_4H_9NH_3)_2(CH_3NH_3)_{n-1}Sn_nI_{3n+1}$) with very promising electronic properties. Lately, the same author explored the electrical, optical and thermal properties of a series of hybrid halide perovskites $(C_4H_9NH_3)_2MI_4$, where M = Ge, Sn or Pb.[39] All these perovskites were synthesized from aqueous hydroiodic acid solutions. MI_4 (M = Ge, Sn and Pb) precursors were dissolved in aqueous HI solutions and reduced to MI_2 by addition of appropriate amounts of H_3PO_3 into the HI solution (Scheme 6). Afterwards, $(C_4H_9NH_3)_2\cdot HI$ solutions in aqueous HI were added to the MI_2 solutions resulting in the formation of the desired perovskites that precipitate from the solution. Orthorhombic structures were obtained for all metals; however, $(C_4H_9NH_3)_2GeI_4$ presented a different space group and greater distortion in the GeI_6 octahedra compared with the perovskites of the other two metals. This distortion produced a lower melting point and smaller bandgap in the $(C_4H_9NH_3)_2GeI_4$ perovskite compared to the other two having Sn and Pb as metals.[39] Although $(C_4H_9NH_3)_2GeI_4$ showed the widest light harvesting ability due to its reduced bandgap, $(C_4H_9NH_3)_2SnI_4$ and $(C_4H_9NH_3)_2PbI_4$ were more stable structures. The similar ionic radii of Sn^{2+} 1.35 Å and Pb^{2+} 1.49 Å result in a lack of significant lattice perturbation in their structures, $(C_4H_9NH_3)_2PbI_4$ exhibiting the bigger bandgap.

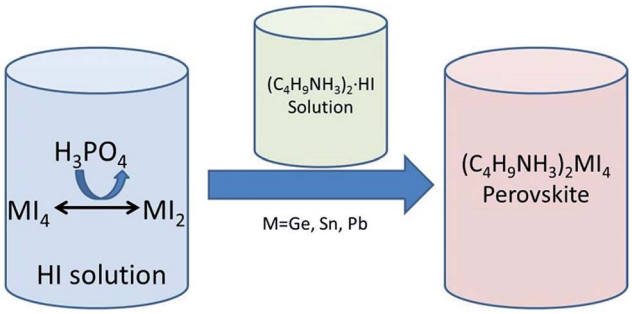

Scheme 6 Preparation procedure of hybrid halide perovskites using Ge, Sn or Pb as metals.

Consequently, the interest in avoiding lead due to environmental concerns as well as extending the light harvesting ability to the NIR boosted the use of hybrid halide perovskites with Sn as a divalent metal cation.[38,40,41] However, this Sn based perovskite has shown a poor stability in air compared with the Pb based perovskite due to the oxidation of Sn^{2+} to Sn^{4+}.

Obviously, this oxidation produces structural changes which are reflected in different properties such as metal-like conductivity and the modification of the performance as a p-type semiconductor.[42] Recently, Ogomi and co-workers found that a minimal content of Pb atoms in the Sn perovskite is enough to decrease the tendency to undergo oxidation from Sn^{2+} to Sn^{4+}, thus increasing perovskite stability in air.[43] In addition, the mix of divalent metal cations (Sn^{2+} and Pb^{2+}) allowed bandgap

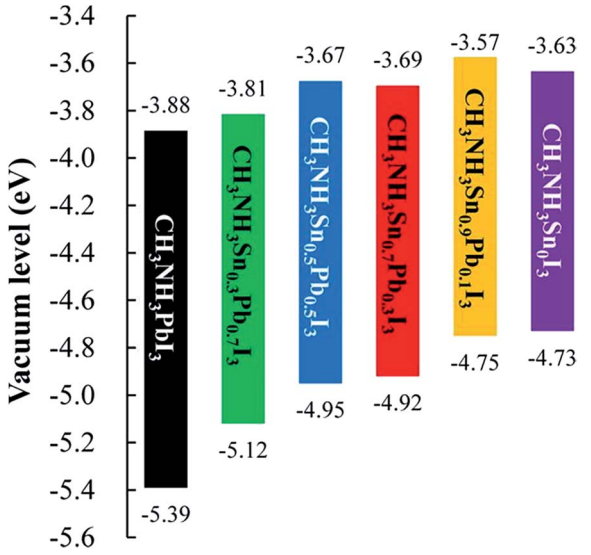

Scheme 7 Energy diagram of $CH_3NH_3Sn_xPb_{(1-x)}I_3$ perovskite. Reproduced with permission from ref. 43.

tuning by varying the Sn : Pb ratio (Scheme 7). Thus, solar cells based on $CH_3NH_3Sn_{0.5}Pb_{0.5}I_3$ perovskite obtained 4.18% efficiency upon 1 Sun illumination and a current density value of 20 mA cm^{-2} was achieved due to the absorption edge of the material at 1060 nm. On the other hand, Kanatzidis *et al.* reported that solid solutions of $CH_3NH_3PbI_3$ and $CH_3NH_3SnI_3$ perovskites achieved 7.27% efficiency for the $CH_3NH_3Pb_{0.5}Sn_{0.5}I_3$ composition.[44] This sample is synthesised by reprecipitation of appropriate amounts of the two different metal perovskites. The difference between the two procedures for preparation of mixed-metal hybrid perovskites is the synthesis procedure. In one case, CH_3NH_3I, PbI_2 and SnI_2 precursors were mixed in stoichiometric proportions to obtain the $CH_3NH_3Sn_{0.5}Pb_{0.5}I_3$ perovskite, while in the latter case the already prepared $CH_3NH_3PbI_3$ and $CH_3NH_3SnI_3$ solids were dissolved together in order to obtain the mixed perovskite with apparently the same composition, but different performance.

Besides the poor air stability observed for the Sn perovskites due to the aerobic Sn^{2+} oxidation, the other problem responsible for the low power conversion efficiency in photovoltaic devices built with Sn-containing perovskites is the discontinuous film morphology and poor electrode coverage (Fig. 1). The inefficient film coverage is responsible for shorting, poor charge transport and fast charge recombination. In this regard, Jen *et al.* reported an improved synthetic route to obtain binary Pb–Sn perovskites.[45] In this report, an ethanolic solution of methylamine was mixed with an aqueous solution of HI in the presence of hydrophosphorous acid. Then, CH_3NH_3I, $PbCl_2$ and $SnCl_2$ were mixed in the desired ratio in anhydrous DMF. Planar heterojunction devices were built using $CH_3NH_3Pb_{1-a}Sn_aI_{3-x}Cl_x$ were prepared in this way and high electrode coverages (up to 97%) were obtained. In addition, the Sn atom incorporation shifted the absorption from 800 nm to 900 nm, achieving a maximum device efficiency of 10.1% at 1 Sun. This result was obtained with 85 : 15 Pb : Sn atomic percentage in the perovskite composition, which correlated with the film with the highest electrode coverage as determined by scanning electron microscopy.[45]

In spite of the enhanced light harvesting in the NIR, and the more than 20 mA cm^{-2} current density obtained from this Sn/Pb mixed perovskite, the overall efficiency under 100 mW cm^{-2} of sun simulated light was still lower than the average efficiency of the Pb based hybrid halide perovskite, although single Pd hybrid perovskite absorbs light only up to 800 nm.

A lower open circuit voltage (V_{oc}) and fill factor (FF) are usually obtained with devices containing Sn in the perovskite structure. Therefore, deeper understanding of the charge transfer reactions taking place in the active layer (especially charge separation and recombination) is needed to devise strategies to overcome these limitations and combine in a material the advantages of the enhanced photocurrent obtained with the Sn based perovskite with the high photovoltage exhibited by Pb based perovskite.

In this regard, Shen and co-workers determined that the density of defects and trap states in binary Sn/Pb perovskites was higher than that in Pb based perovskites.[46] As a consequence, only 20% of the Sn/Pb based perovskite excited states have lifetime longer than 3 ns (Fig. 2), while, in Pb based perovskite 90% of excitons decayed after 100 ns. This faster excited state deactivation was attributed to nonradiative charge recombination through trap states in the binary perovskite. The authors found it possible to enhance the V_{oc} and FF by defect density reduction in the Sn/Pb perovskites.[46] Therefore, composition optimization and engineering of the Sn based perovskite are needed in order to reduce the density of defects and reduce recombination.

One example of composition engineering can be found in the case of an all inorganic $CsSnI_3$ perovskite with an orthorhombic structure, which has been employed as a solid electrolyte in a dye-sensitized solar cell.[47] The typical I^-/I_3^- redox pair in liquid electrolytes can be replaced with this inorganic perovskite, which not only presented improved hole mobility properties, respect to other solid state electrolytes, but also its 1.3 eV bandgap introduces additional photoresponse in the NIR part of the radiation spectra (absorption edge 953 nm). Photovoltaic devices employing this perovskite as the solid electrolyte achieved more than 10% efficiency by doping the perovskite

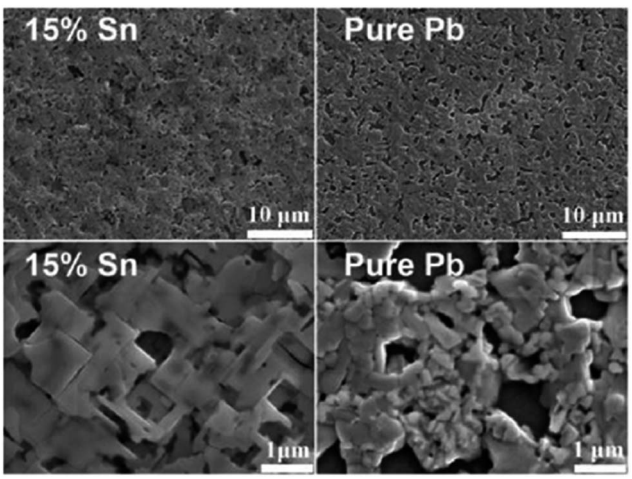

Fig. 1 SEM images of $CH_3NH_3Pb_x$ (right) and $CH_3NH_3Pb_{0.85}Sn_{0.15}X$ (left) films. Reproduced with permission from ref. 45.

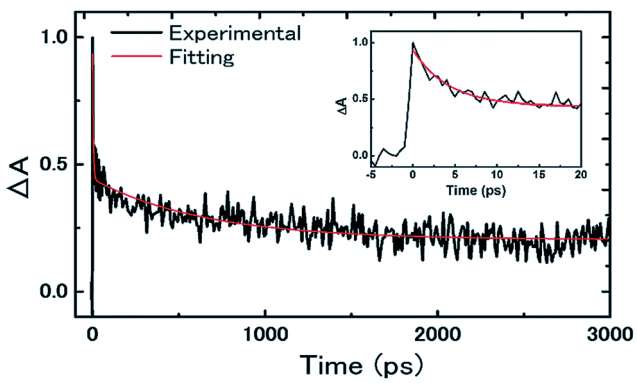

Fig. 2 Transient absorption response of Sn/Pb perovskite on the Al_2O_3 substrate (black: experimental signal; red: best fitting). The inset shows the transient signal for the first 20 ps. Reproduced with permission from ref. 46.

with 5% of F^- ($CsSnI_{2.9}F_5$).[47] Based on this precedent, $CsSnI_3$ has also been employed as an active material in solar cells with spectral responses up to 950 nm. Nevertheless, efficient photovoltaic devices were only obtained by doping the inorganic perovskite with SnF_2. The poor performance without the F^- doping was due to the presence of intrinsic defects associated with the Sn metal cation, which results in metallic conductivity. Therefore, the addition of SnF_2 was found to be very important in order to reduce background carrier density.[48]

Theoretical calculations have revealed that the main differences between Sn and Pb based perovskites are a consequence of relativistic effects due to the contraction of valence band atomic orbitals. These effects stabilize significantly Pb based perovskites against oxidation due to the much deeper valence band edge, which at the same time also increases their bandgap.[49] In other words, theory indicates that the optimum Sn based perovskite bandgap derives from a relatively elevated valence band that, on the other hand, is also responsible for the easy Sn^{2+} oxidation.

Other candidates for lead-free perovskites such as $(CH_3NH_3)_2CuCl_{4-x}Br_x$ or $(RNH_3)_2FeX_4$ have been synthesized.[50,51] However in these cases 2H structures have been obtained instead of the 3D polymorphs resulting for metals from the 14 group. In the case of the Cu based perovskite the bandgap can be tuned by increasing the ratio of Br in the structure. However, the presence of Cl has been found to be crucial in order to avoid Cu^{2+} reduction. Although light harvesting in the NIR region has been achieved, efficiencies as low as 0.02% were measured and attributed to the partial Cu^{2+} reduction by Br^-, which introduces anion vacancies acting as charge carrier trapping sites.[50] In the case of the Fe based perovskites metal oxidation from Fe^{2+} to Fe^{3+} has been identified as a possible source of instability, and there are still no optoelectronic studies showing the photovoltaic activity of Fe hybrid halide perovskites in spite of their obvious interest derived from abundance and the lack of toxicity of Fe.[7]

The synthesis and crystallographic characterization of $NH_3(C_6H_4)_2NH_3CuCl_4$ and $NH_3(C_6H_4)_2NH_3HgCl_4$ organic–inorganic perovskites have been also reported.[52] The Cu based perovskite structure showed well-ordered sheets of corner-sharing distorting $CuCl_6$ octahedra, separated by layers of the organic cation. However, the Hg based perovskite presented anionic parallel layers and alternating layers of the organic cation and tetrahedral $HgCl_4^{2-}$. In both cases, the different organic–inorganic layers are interconnected by relatively weak H-bonds between amino groups of organic cations and the Cl^- of the anionic counterparts,[52] making them good candidates to explore their photovoltaic performance or for the synthesis of similar structures containing organic cations with different compositions and sizes.

In this regard, Papavassiliou *et al.* reported a complete structural, optical and electronic study of organic–inorganic semiconductors using combinations of a wide range of organic cations and metal halides (M = Bi, Sb, Sn, Pb, Cu and Ag),[53] opening the possibility to explore the use of metal alternatives to Pb.

The inorganic anion

As commented earlier, many perovskites of different compositions have been described in the literature (oxides, nitrides or halides). However, hybrid halide perovskites have been found to exhibit the best optoelectronic properties. In this regard, the influence of the halogen elements I, Cl and Br, and their combinations has been widely studied and a strong dependence of the photovoltaic performance of the perovskite cell depending on the halogen composition has been demonstrated.

It was reported in 2003 that $CH_3NH_3PbBr_3$ presented a larger bandgap and tighter bound excitons than $CH_3NH_3PbI_3$ as a consequence of the intrinsic properties of each halogen.[54] Exciton binding energies of 76 meV and 50 meV were estimated for $CH_3NH_3PbBr_3$ and $CH_3NH_3PbI_3$, respectively, which are larger than the exciton binding energy of other inorganic semiconductors such as GaAs (4.2 meV).[55] This was lately confirmed in perovskite solar cells, where the hybrid halide perovskites $CH_3NH_3PbI_3$ and $CH_3NH_3PbBr_3$ were compared using liquid electrolytes.[1] The power conversion efficiencies of $CH_3NH_3PbI_3$ and $CH_3NH_3PbBr_3$ were 3.81% and 3.18%, respectively. However, to put these efficiency values in perspective it has to be considered that perovskites containing I showed a smaller bandgap than perovskites containing Br. Therefore, in the incident photon to current efficiency (IPCE) measurements, it was determined that devices based on $CH_3NH_3PbI_3$ harvested light up to 800 nm, while in $CH_3NH_3PbBr_3$ devices light harvesting occurs below 600 nm. When corrected for this difference in light absorption, the differences in IPCE values are very minor. In addition, photoelectron spectroscopy determined that the $CH_3NH_3PbI_3$ valence band (5.44 eV) is higher in energy than the $CH_3NH_3PbBr_3$ valence band (5.38 eV) and conduction band edges calculated from the valence band and the optical bandgap were estimated to be at 3.36 eV for $CH_3NH_3PbBr_3$ and 4 eV for $CH_3NH_3PbI_3$.[1] The origin of the V_{oc} in perovskite based photovoltaic devices still remains unclear and it is under discussion. Although active materials showing larger band gaps should, in principle, lead to devices with higher V_{oc} than smaller band gaps materials due to the energy difference between their conduction and valence bands, the redox potential of organic hole conductors and the work function of the different electrodes used in device construction, together with internal resistance, limit the observed V_{oc} in devices. The recombination rate plays a key role in the performance not only in perovskite solar cells but also in other types of photovoltaic devices such as dye sensitized solar cells or organic solar cells. Recombination dynamics has been found to be composition-dependent in perovskite solar cells, and the addition of a small percentage of Br^- into mixed halides perovskite solar cells has been found to reduce the recombination rate when compared to the pure materials.[56]

The high band gap in $CH_3NH_3PbBr_3$ perovskites allows the possibility to build high V_{oc} solar cells, which could offer opportunities in electrochemical reactions,[57,58] tandem cells[59] or photodetectors.[60] In this sense Qiu and co-workers reported hybrid $CH_3NH_3PbBr_3$ perovskite solar cells exhibiting 1.15 V at

open circuit using poly[*N*-9-heptadecanyl-2,7-carbazole-*alt*-3,6-bis-(thiophen-5-yl)-2,5-dioctyl-2,5-di-hydropyrrolo[3,4]pyrrole-1,4-dione] (PCBTDPP) as a hole conductor. Similarly, others reports have appeared showing the use of different hole conductors in $CH_3NH_3PbBr_3$ perovskite solar cells in order to maximize the open circuit voltage up to 1.4 V.[61,62]

In spite of the high open circuit voltages obtained with the Br perovskite and the reported organic hole conductors, the overall efficiencies obtained at 1 Sun illumination in such devices were far from the average efficiency obtained using I as an inorganic anion in the perovskite. This low efficiency makes difficult the application of bromide-based perovskite in the production of solar fuels or tandem cells. However, Im *et al.* reported that one of the reasons for such a low efficiency could be a low density of $CH_3NH_3PbBr_3$ films, and therefore, poor electrode coverage.[63] They found that $CH_3NH_3PbBr_3$ perovskite dissolved in DMF produced fast nucleation of isolated $CH_3NH_3PbBr_3$ crystals, which produced low coverage and inefficient devices. However, when they added HBr aqueous solution to the $CH_3NH_3PbBr_3$ perovskite in DMF the crystal nucleation slowed down, due to the improved solubility of $CH_3NH_3PbBr_3$ in the solvent mix, resulting in the formation of denser and thinner films with full coverage. Using the DMF/HBr solvent and the organic hole conductor PIF8-TAA, 10.4% efficiency at 1 Sun illumination was obtained, exhibiting 1.5 V in open circuit.[63] Recently, a vapor-assisted method for $CH_3NH_3PbBr_3$ fabrication has been utilized as an alternative to overcome the poor film coverage that solution methods present. A $PbBr_2$ film, previously deposited by spin coating, was treated with CH_3NH_3Br vapor at 150 °C for 10 min. This procedure allowed densely packed grains and full film coverage on a transparent electrode which produced 8.7% efficiency with 1.45 V_{oc} at 1 Sun.[64]

Theoretical calculations have determined that defects in $CH_3NH_3PbBr_3$ are predominantly shallow traps,[65] suggesting negligible losses due to non-radiative recombination pathways. These calculations are in agreement with the observation of the high open circuit voltages in $CH_3NH_3PbBr_3$ perovskite solar cells. However, these calculations indicate that $CH_3NH_3PbBr_3$ should exhibit only unipolar behavior and, therefore, it can only act as a p-type semiconductor in contrast to the $CH_3NH_3PbI_3$, which shows bipolar behavior. Therefore, the less efficient electron transport determines that optimal $CH_3NH_3PbBr_3$ perovskite films have to be thinner than $CH_3NH_3PbI_3$ for balanced electron/hole extraction, losing under these conditions light harvesting ability. Thus, a compromise between light absorption and the optimal film thickness appears to be crucial for the best performing $CH_3NH_3PbBr_3$ perovskite cell. Poor charge migration should be responsible for enhanced charge recombination in $CH_3NH_3PbBr_3$ compared with $CH_3NH_3PbI_3$ perovskite solar cells. Nevertheless, $CH_3NH_3PbBr_3$ has been proposed as a good candidate for the top cells in tandem solar cells, being an excellent additive for light harvesting in other perovskite solar cells to achieve high photovoltage, as well as for hole transport.[65]

The $CH_3NH_3PbCl_3$ perovskite presents an even higher bandgap (3.11 eV) than $CH_3NH_3PbBr_3$ perovskites (2.3 eV) and $CH_3NH_3PbI_3$ (1.55 eV). For that reason $CH_3NH_3PbCl_3$ cannot be used as a light harvesting material. However, the use of mixed halide perovskites appears as a promising approach to tune the optoelectronic properties of single halide perovskites, improving the photovoltaic performance of single-halide perovskite solar cells. The incorporation of mixed halide anions into the structure of the archetypical $CH_3NH_3PbI_3$ hybrid perovskite has been found to affect the charge recombination dynamics in the photovoltaic devices. Mora-Sero *et al.* determined that the incorporation of Cl^- or Br^- into the perovskite structure slows down recombination kinetics, increasing the V_{oc}. In addition, the presence of Br improved the device stability.[56] Nevertheless, the role of Cl anions and how many of them remain in the final structure of the mixed halide perovskite are still under discussion.[66,67] In any case, incorporation of Cl^- into the composition of perovskite solar cells has proved to extend the charge diffusion length without changing the spectral response, although only a small percentage of Cl atoms can be tolerated in the perovskite lattice.

In 2012, Snaith *et al.* reported the use of a $CH_3NH_3PbI_{3-x}Cl_x$ perovskite using either TiO_2 or Al_2O_3 as an n-type component or scaffold, respectively.[2] They found that devices using an Al_2O_3 mesoporous layer were more efficient than those using TiO_2, mainly due to the faster electron transport in the mixed perovskite when Al_2O_3 was used instead of TiO_2. Apart from device structural considerations, they found that the crystallization rate can be controlled by changing the halide composition. The inclusion of Cl atoms replacing a percentage of I produced a longer crystallization process as a consequence of lattice distortion generated by the Cl inclusion in the perovskite structure. Moreover, I anion substitution by Cl was again found to increase the electron conductivity and charge diffusion length. These beneficial effects seem to be not counterbalanced by important negative side effects in the film since spectroscopic measurements have shown similar light harvesting (from 400 to 800 nm) for $NH_3NH_3PbI_{3-x}Cl_x$ compared to the parent $CH_3NH_3PbI_3$ perovskite solar cells, indicating no change in bandgap (1.55 eV) despite the incorporation of Cl into the perovskite lattice. The use of the mixed halide $CH_3NH_3PbI_{3-x}Cl_x$ not only produces a remarkable enhancement in the film conductivity, but also improves the morphology of the films in comparison with those of $CH_3NH_3PbI_3$ devices processed under the same conditions. Other additional benefits are the reduction of the *J–V* hysteresis and an improvement in the device reproducibility.[68,69]

Crystallization is an important process controlling the overall photovoltaic cell performance that depends on multiple variables such as precursor composition, concentration, solvents and deposition temperature. In this regard, highly dense films of mixed halide perovskite $CH_3NH_3PbI_{3-x}Cl_x$ have been deposited *via* the solution processing method resulting in highly reproducible photovoltaic devices with efficiencies up to 10.8%.[70] These dense films were achieved by increasing the mixed halide perovskite precursor concentrations and optimizing film deposition conditions by controlling the spin rate. Both modifications were carried out by using dimethyl sulfoxide (DMSO) as the solvent, since compared with DMF or mixed DMF and γ-butyrolactone, DMSO allows preparation of more

concentrated $CH_3NH_3PbI_{3-x}Cl_x$ precursors (up to 60 wt%). In addition, DMSO possesses a higher boiling point which is advantageous for achieving a slower drying.[70] Other approaches employed to control the crystal growth in solution processed mixed halide perovskites are based on the use of additives (such as 1,8-diiodooctane) in the precursor solutions.[71]

The formation of flat uniform films of $CH_3NH_3PbI_{3-x}Cl_x$ using a dual-source vapor deposition method has been also demonstrated by Snaith *et al.*[14] In this way, planar heterojunction photovoltaic devices were prepared, demonstrating 15% efficiency at 1 Sun, without the need for using solvents and subsequent drying. Using this preparation method, an orthorhombic structure of high crystal quality was reported, having in the XRD pattern smaller peaks attributable to PbI_2, in contrast to the patterns obtained from solution processing methods. In addition, no peaks corresponding to $CH_3NH_3PbCl_3$ were found.

Besides I and Cl mixed halide perovskites, other halide mixtures have been tested in perovskite solar cells. For example, $CH_3NH_3PbI_2Br$ has been deposited on TiO_2 nanowires and compared with the $CH_3NH_3PbI_3$ perovskite in photovoltaic devices. The Br introduction into the perovskite lattice produced a higher absorption coefficient and shifted the conduction band to higher energy values. As a consequence, both the power conversion efficiency and open circuit voltage of the mixed halide perovskite were improved in comparison with the parent $CH_3NH_3PbI_3$ perovskite devices.[72] In fact, Seok *et al.* tuned the optical and electronic properties of $CH_3NH_3Pb(I_{1-x}Br_x)_3$ by composition engineering. They controlled the perovskite bandgap over almost the complete visible region, changing the I/Br ratio, and obtaining 12.3% power conversion for the most efficient photovoltaic devices containing a mixed halide perovskite with $x = 0.2$.[73]

As commented earlier, the $CH_3NH_3PbBr_3$ perovskite is a wide bandgap material with excellent hole conducting properties. Therefore, this perovskite has been used in combination with $CH_3NH_3PbI_3$ in order to obtain, on one hand, tunable bandgap perovskite, and on the other hand, free hole conductor perovskite solar cells.[74]

High voltage perovskite solar cells have been reported using the mixed halide perovskite $CH_3NH_3PbBr_{3-x}Cl_x$.[75] The inclusion of Cl anions in the $CH_3NH_3PbBr_3$ perovskite produced not only an enhancement in the V_{oc}, but also in J_{sc}. Thus, values of 1.5 V and 4 mA cm^{-2} were observed for this $CH_3NH_3PbBr_{3-x}Cl_x$ perovskite upon 100 mW cm^{-2} irradiation at 1 Sun. The enhanced V_{oc} and J_{sc} with respect to the Br^- only based perovskite were attributed to an improved film coverage caused by the presence of the Cl^- anions, increasing in this way the light absorption and decreasing losses due to shorting. It was observed that the presence of Cl^- produces smaller crystallites, which results in a denser perovskite layer.[75] Actually, crystallization studies have determined that the inclusion of $PbCl_2$ during the formation of both $CH_3NH_3PbI_3$ and $CH_3NH_3PbBr_3$ perovskites has a beneficial effect on the quality of the final perovskite layers since $PbCl_2$ crystals act as nucleation points during perovskite formation due to its low solubility in DMF that is the common solvent used. $PbCl_2$ activity as seeds results in more dense layers for both I and Br perovskites obtained when $PbCl_2$ is added.[76]

Apart from Cl and Br anions, F^- has been also incorporated into the structure of mixed halide perovskites by Nagane and coworkers.[77] They reported the partial substitution of I^- by BF_4^- anions, which present a similar ionic radius. It was reported before that the stability of the perovskite structure decreases from I^- to F^-, making the formation of stable F^- and I^- mixed halide perovskites really difficult.[78] However, the preparation of $CH_3NH_3PbI_{(3-x)}(BF_4)_x$ through chemical vapor deposition of the prepared $CH_3NH_3BF_4$ on PbI_2 films produced tetragonal crystal structures identical to the typical $CH_3NH_3PbI_3$. The incorporation of F atoms into the BF_4^- anion produced an enhanced conductivity in the perovskite films. This was explained in terms of the higher electronegativity and electron withdrawing behavior of F compared with the other halides. Besides, the F^- radius is smaller than that of I^-; therefore the substitution of I^- directly by F^- rather than by BF_4^- should result, in the case of Pb, in strong lattice deformation resulting in detrimental optoelectronic consequences. However, the incorporation of the F atoms into the BF_4^- anion, with a similar ionic radius to I^-, avoids this lattice distortion and induces improved electrical conductivity, maintaining an absorption edge at 760 nm.[77]

Conclusions

Perovskite solar cells have abruptly emerged in the photovoltaic field due to the high power conversion efficiency they demonstrated in just few years. This breakthrough in the photovoltaic field is a consequence, on one hand, of the considerable structural and chemical knowledge of hybrid perovskites that started decades ago by Weber,[79] and lately, the study of their physical properties by Mitzi.[37–40] On the other hand, the technological advances in the preparation of films and deposition methods, already developed for other photovoltaic technologies, have been adapted in a straightforward manner for the preparation of perovskite solar cells.

$CH_3NH_3PbI_3$ perovskite solar cells have demonstrated impressive record device efficiencies, and almost introduction in the commercial market has already been informed.[80] The now-a-days efficiency is getting close to the theoretical maximum value (~31%), which is close to the Shockley and Queisser limit of 33%.[81] This theoretical limit predicts a maximum J_{sc} of 26 mA cm^{-2} and V_{oc} of 1.3 V, approximately.[82] Nevertheless, some open questions and concerns still require further research and developments such as the origin of the hysteresis effect in the *J–V* curves measurements, which causes doubts in the accuracy of the efficiency measurements, the need for lead-free perovskites to avoid the use of this toxic heavy metal and the long-term stability demonstration of such photovoltaic technology.

In this regard, variation of the chemical composition of the hybrid halide perovskites can be a suitable methodology for finding an adequate solution for these three targets. The substitution of the typical methylammonium organic cation has been proved to extend light absorption into the NIR region, enhancing at the same time the crystal phase and material stability. The search for new organic or even inorganic cations

with similar radii to that of the ammonium cation could open new possibilities to improve even further the optoelectronic performance that hybrid perovskites have shown so far. Moreover, it has been demonstrated that the partial substitution of the Pb cation by Sn, besides reducing the amount of undesirable Pb toxic metal, is able to allow certain bandgap tuning, achieving absorption edge up to 1060 nm. The search for new metal cations with similar properties to those corresponding to the 14 group is still open, and some perovskites containing Cu or Fe have been already prepared, although the currently available performance data are far from optimal. Finally, the use of mixed halide perovskites has been found to improve film coverage, allowing also tuning of the perovskite bandgap, disfavoring charge recombination events and even improving stability. Nonetheless, not only halides must be tested in photovoltaic applications, but also other counter anions susceptible to form perovskite structures (as nitrates or oxides) should be tested in order to achieve higher device stability and efficiencies that currently limit the commercial application of hybrid perovskite photovoltaic solar cells.

Acknowledgements

Financial support by the Spanish Ministry of Economy and Competitiveness (Severo Ochoa and CTQ2015-69153-C2-1-R) and Generalidad Valenciana (Prometeo 2013/014) is gratefully acknowledged.

References

1 A. Kojima, K. Teshima, Y. Shirai and T. Miyasaka, *J. Am. Chem. Soc.*, 2009, **131**, 6050–6051.
2 M. M. Lee, J. Teuscher, T. Miyasaka, T. N. Murakami and H. J. Snaith, *Science*, 2012, **338**, 643–647.
3 H. Zhou, Q. Chen, G. Li, S. Luo, T.-b. Song, H.-S. Duan, Z. Hong, J. You, Y. Liu and Y. Yang, *Science*, 2014, **345**, 542–546.
4 National Renewable Energy Labs (NREL) Efficiency Chart.
5 N. J. Jeon, J. H. Noh, W. S. Yang, Y. C. Kim, S. Ryu, J. Seo and S. I. Seok, *Nature*, 2015, **517**, 476–480.
6 S. D. Stranks, P. K. Nayak, W. Zhang, T. Stergiopoulos and H. J. Snaith, *Angew. Chem., Int. Ed.*, 2015, **54**, 3240–3248.
7 P. P. Boix, S. Agarwala, T. M. Koh, N. Mathews and S. G. Mhaisalkar, *J. Phys. Chem. Lett.*, 2015, **6**, 898–907.
8 S. Luo and W. A. Daoud, *J. Mater. Chem. A*, 2015, **3**, 8992–9010.
9 V. M. Burlakov, G. E. Eperon, H. J. Snaith, S. J. Chapman and A. Goriely, *Appl. Phys. Lett.*, 2014, **104**, 091602.
10 N.-G. Park, *Mater. Today*, 2015, **18**, 65–72.
11 G. E. Eperon, V. M. Burlakov, P. Docampo, A. Goriely and H. J. Snaith, *Adv. Funct. Mater.*, 2014, **24**, 151–157.
12 E. L. Unger, E. T. Hoke, C. D. Bailie, W. H. Nguyen, A. R. Bowring, T. Heumuller, M. G. Christoforo and M. D. McGehee, *Energy Environ. Sci.*, 2014, **7**, 3690–3698.
13 T. Leijtens, B. Lauber, G. E. Eperon, S. D. Stranks and H. J. Snaith, *J. Phys. Chem. Lett.*, 2014, **5**, 1096–1102.
14 M. Liu, M. B. Johnston and H. J. Snaith, *Nature*, 2013, **501**, 395–398.
15 N. J. Jeon, J. H. Noh, Y. C. Kim, W. S. Yang, S. Ryu and S. I. Seok, *Nat. Mater.*, 2014, **13**, 897–903.
16 N. Ahn, D.-Y. Son, I.-H. Jang, S. M. Kang, M. Choi and N.-G. Park, *J. Am. Chem. Soc.*, 2015, **137**, 8696–8699.
17 D. Liu and T. L. Kelly, *Nat. Photonics*, 2014, **8**, 133–138.
18 Q. Chen, H. Zhou, Z. Hong, S. Luo, H.-S. Duan, H.-H. Wang, Y. Liu, G. Li and Y. Yang, *J. Am. Chem. Soc.*, 2014, **136**, 622–625.
19 Z. Xiao, C. Bi, Y. Shao, Q. Dong, Q. Wang, Y. Yuan, C. Wang, Y. Gao and J. Huang, *Energy Environ. Sci.*, 2014, **7**, 2619–2623.
20 J. Burschka, N. Pellet, S.-J. Moon, R. Humphry-Baker, P. Gao, M. K. Nazeeruddin and M. Gratzel, *Nature*, 2013, **499**, 316–319.
21 Y. Zhao and K. Zhu, *J. Phys. Chem. Lett.*, 2014, **5**, 4175–4186.
22 J. J. Choi, X. Yang, Z. M. Norman, S. J. L. Billinge and J. S. Owen, *Nano Lett.*, 2014, **14**, 127–133.
23 L. Zheng, D. Zhang, Y. Ma, Z. Lu, Z. Chen, S. Wang, L. Xiao and Q. Gong, *Dalton Trans.*, 2015, **44**, 10582–10593.
24 T. Baikie, Y. Fang, J. M. Kadro, M. Schreyer, F. Wei, S. G. Mhaisalkar, M. Graetzel and T. J. White, *J. Mater. Chem. A*, 2013, **1**, 5628–5641.
25 G. Kieslich, S. Sun and A. K. Cheetham, *Chem. Sci.*, 2014, **5**, 4712–4715.
26 A. Amat, E. Mosconi, E. Ronca, C. Quarti, P. Umari, M. K. Nazeeruddin, M. Grätzel and F. De Angelis, *Nano Lett.*, 2014, **14**, 3608–3616.
27 J.-W. Lee, D.-J. Seol, A.-N. Cho and N.-G. Park, *Adv. Mater.*, 2014, **26**, 4991–4998.
28 G. E. Eperon, S. D. Stranks, C. Menelaou, M. B. Johnston, L. M. Herz and H. J. Snaith, *Energy Environ. Sci.*, 2014, **7**, 982–988.
29 S. Pang, H. Hu, J. Zhang, S. Lv, Y. Yu, F. Wei, T. Qin, H. Xu, Z. Liu and G. Cui, *Chem. Mater.*, 2014, **26**, 1485–1491.
30 J.-H. Im, J. Chung, S.-J. Kim and N.-G. Park, *Nanoscale Res. Lett.*, 2012, **7**, 353.
31 T. M. Koh, K. Fu, Y. Fang, S. Chen, T. C. Sum, N. Mathews, S. G. Mhaisalkar, P. P. Boix and T. Baikie, *J. Phys. Chem. C*, 2014, **118**, 16458–16462.
32 W. S. Yang, J. H. Noh, N. J. Jeon, Y. C. Kim, S. Ryu, J. Seo and S. I. Seok, *Science*, 2015, **348**, 1234–1237.
33 N. Pellet, P. Gao, G. Gregori, T.-Y. Yang, M. K. Nazeeruddin, J. Maier and M. Grätzel, *Angew. Chem., Int. Ed.*, 2014, **53**, 3151–3157.
34 A. Mei, X. Li, L. Liu, Z. Ku, T. Liu, Y. Rong, M. Xu, M. Hu, J. Chen, Y. Yang, M. Grätzel and H. Han, *Science*, 2014, **345**, 295–298.
35 M. Kulbak, D. Cahen and G. Hodes, *J. Phys. Chem. Lett.*, 2015, 2452–2456.
36 H. Choi, J. Jeong, H.-B. Kim, S. Kim, B. Walker, G.-H. Kim and J. Y. Kim, *Nano Energy*, 2014, **7**, 80–85.
37 D. B. Mitzi, in *Progress in Inorganic Chemistry*, John Wiley & Sons, Inc., 2007, pp. 1–121.
38 D. B. Mitzi, C. A. Feild, W. T. A. Harrison and A. M. Guloy, *Nature*, 1994, **369**, 467–469.
39 D. B. Mitzi, *Chem. Mater.*, 1996, **8**, 791–800.
40 D. B. Mitzi, S. Wang, C. A. Feild, C. A. Chess and A. M. Guloy, *Science*, 1995, **267**, 1473–1476.

41 N. K. Noel, S. D. Stranks, A. Abate, C. Wehrenfennig, S. Guarnera, A.-A. Haghighirad, A. Sadhanala, G. E. Eperon, S. K. Pathak, M. B. Johnston, A. Petrozza, L. M. Herz and H. J. Snaith, *Energy Environ. Sci.*, 2014, **7**, 3061–3068.
42 C. C. Stoumpos, C. D. Malliakas and M. G. Kanatzidis, *Inorg. Chem.*, 2013, **52**, 9019–9038.
43 Y. Ogomi, A. Morita, S. Tsukamoto, T. Saitho, N. Fujikawa, Q. Shen, T. Toyoda, K. Yoshino, S. S. Pandey, T. Ma and S. Hayase, *J. Phys. Chem. Lett.*, 2014, **5**, 1004–1011.
44 F. Hao, C. C. Stoumpos, R. P. H. Chang and M. G. Kanatzidis, *J. Am. Chem. Soc.*, 2014, **136**, 8094–8099.
45 F. Zuo, S. T. Williams, P.-W. Liang, C.-C. Chueh, C.-Y. Liao and A. K. Y. Jen, *Adv. Mater.*, 2014, **26**, 6454–6460.
46 Q. Shen, Y. Ogomi, J. Chang, T. Toyoda, K. Fujiwara, K. Yoshino, K. Sato, K. Yamazaki, M. Akimoto, Y. Kuga, K. Katayama and S. Hayase, *J. Mater. Chem. A*, 2015, **3**, 9308–9316.
47 I. Chung, B. Lee, J. He, R. P. H. Chang and M. G. Kanatzidis, *Nature*, 2012, **485**, 486–489.
48 M. H. Kumar, S. Dharani, W. L. Leong, P. P. Boix, R. R. Prabhakar, T. Baikie, C. Shi, H. Ding, R. Ramesh, M. Asta, M. Graetzel, S. G. Mhaisalkar and N. Mathews, *Adv. Mater.*, 2014, **26**, 7122–7127.
49 P. Umari, E. Mosconi and F. De Angelis, *Sci. Rep.*, 2014, **4**, 04467.
50 D. Cortecchia, H. Arianita Dewi, D. Sabba, T. Baikie, C. Soci and N. Mathews, in *EOSAM 2014*, European Optical Society, Berlin, 2014.
51 M. F. Mostafa, M. A. Semary and M. A. Ahmed, *Phys. Lett. A*, 1977, **61**, 183–184.
52 M. Belhouchet, W. Wamani and T. Mhiri, *IOP Conf. Ser.: Mater. Sci. Eng.*, 2010, **13**, 012039.
53 G. C. Papavassiliou, G. A. Mousdis and I. B. Koutselas, *Adv. Mater. Opt. Electron.*, 1999, **9**, 265–271.
54 K. Tanaka, T. Takahashi, T. Ban, T. Kondo, K. Uchida and N. Miura, *Solid State Commun.*, 2003, **127**, 619–623.
55 S. B. Nam, D. C. Reynolds, C. W. Litton, R. J. Almassy, T. C. Collins and C. M. Wolfe, *Phys. Rev. B: Solid State*, 1976, **13**, 761–767.
56 B. Suarez, V. Gonzalez-Pedro, T. S. Ripolles, R. S. Sanchez, L. Otero and I. Mora-Sero, *J. Phys. Chem. Lett.*, 2014, **5**, 1628–1635.
57 T. Hisatomi, J. Kubota and K. Domen, *Chem. Soc. Rev.*, 2014, **43**, 7520–7535.
58 M. G. Walter, E. L. Warren, J. R. McKone, S. W. Boettcher, Q. Mi, E. A. Santori and N. S. Lewis, *Chem. Rev.*, 2010, **110**, 6446–6473.
59 S. Rühle, A. Segal, A. Vilan, S. R. Kurtz, L. Grinis, A. Zaban, I. Lubomirsky and D. Cahen, *J. Renewable Sustainable Energy*, 2009, **1**, 013106.
60 G. Konstantatos, I. Howard, A. Fischer, S. Hoogland, J. Clifford, E. Klem, L. Levina and E. H. Sargent, *Nature*, 2006, **442**, 180–183.
61 E. Edri, S. Kirmayer, D. Cahen and G. Hodes, *J. Phys. Chem. Lett.*, 2013, **4**, 897–902.
62 S. Ryu, J. H. Noh, N. J. Jeon, Y. Chan Kim, W. S. Yang, J. Seo and S. I. Seok, *Energy Environ. Sci.*, 2014, **7**, 2614–2618.
63 J. H. Heo, D. H. Song and S. H. Im, *Adv. Mater.*, 2014, **26**, 8179–8183.
64 R. Sheng, A. Ho-Baillie, S. Huang, S. Chen, X. Wen, X. Hao and M. A. Green, *J. Phys. Chem. C*, 2015, **119**, 3545–3549.
65 T. Shi, W.-J. Yin, F. Hong, K. Zhu and Y. Yan, *Appl. Phys. Lett.*, 2015, **106**, 103902.
66 M. Gratzel, *Nat. Mater.*, 2014, **13**, 838–842.
67 S. A. Bretschneider, J. Weickert, J. A. Dorman and L. Schmidt-Mende, *APL Mater.*, 2014, **2**, 040701.
68 S. Dharani, H. A. Dewi, R. R. Prabhakar, T. Baikie, C. Shi, D. Yonghua, N. Mathews, P. P. Boix and S. G. Mhaisalkar, *Nanoscale*, 2014, **6**, 13854–13860.
69 Q. Chen, H. Zhou, Y. Fang, A. Z. Stieg, T.-B. Song, H.-H. Wang, X. Xu, Y. Liu, S. Lu, J. You, P. Sun, J. McKay, M. S. Goorsky and Y. Yang, *Nat. Commun.*, 2015, **6**, 7269.
70 B. Conings, L. Baeten, C. De Dobbelaere, J. D'Haen, J. Manca and H.-G. Boyen, *Adv. Mater.*, 2014, **26**, 2041–2046.
71 P.-W. Liang, C.-Y. Liao, C.-C. Chueh, F. Zuo, S. T. Williams, X.-K. Xin, J. Lin and A. K. Y. Jen, *Adv. Mater.*, 2014, **26**, 3748–3754.
72 J. Qiu, Y. Qiu, K. Yan, M. Zhong, C. Mu, H. Yan and S. Yang, *Nanoscale*, 2013, **5**, 3245–3248.
73 J. H. Noh, S. H. Im, J. H. Heo, T. N. Mandal and S. I. Seok, *Nano Lett.*, 2013, **13**, 1764–1769.
74 S. Aharon, B. E. Cohen and L. Etgar, *J. Phys. Chem. C*, 2014, **118**, 17160–17165.
75 E. Edri, S. Kirmayer, M. Kulbak, G. Hodes and D. Cahen, *J. Phys. Chem. Lett.*, 2014, **5**, 429–433.
76 Y. Tidhar, E. Edri, H. Weissman, D. Zohar, G. Hodes, D. Cahen, B. Rybtchinski and S. Kirmayer, *J. Am. Chem. Soc.*, 2014, **136**, 13249–13256.
77 S. Nagane, U. Bansode, O. Game, S. Chhatre and S. Ogale, *Chem. Commun.*, 2014, **50**, 9741–9744.
78 E. Mosconi, A. Amat, M. K. Nazeeruddin, M. Grätzel and F. De Angelis, *J. Phys. Chem. C*, 2013, **117**, 13902–13913.
79 D. Weber, *Z. Naturforsch., B: Anorg. Chem., Org. Chem.*, 1978, **33**, 1443–1445.
80 http://optics.org/news/6/6/21, Imec presents perovskite photovoltaic module with 8% power conversion efficiency.
81 W. Shockley and H. J. Queisser, *J. Appl. Phys.*, 1961, **32**, 510–519.
82 W. E. I. Sha, X. Ren, L. Chen and W. C. H. Choy, *Appl. Phys. Lett.*, 2015, **106**, 221104.